

Invited Contribution from Recipient of ACS Award in Pure Chemistry

Programming the Assembly of Two- and Three-Dimensional Architectures with DNA and Nanoscale Inorganic Building Blocks^{†,‡}

Chad A. Mirkin

Department of Chemistry, Northwestern University, Evanston, Illinois 60208-3113

Received September 20, 1999

The use of biochemical molecular recognition principles for the assembly of nanoscale inorganic building blocks into macroscopic functional materials constitutes a new frontier in science. This article details efforts pertaining to the use of sequence-specific DNA hybridization events and novel inorganic surface coordination chemistry to control the formation of both two- and three-dimensional functional architectures.

Today, I want to tell you about a couple of projects that our group has been developing over the past few years, both of which deal with the general area of nanotechnology. We are very excited about this work because we think it will lead to a general methodology for preparing nanostructured materials with predefined, synthetically programmable properties from common inorganic building blocks and readily available DNA interconnect molecules. The intellectual payoffs from this work will be a greater understanding of (1) the collective interactions between nanoscale building blocks in the context of organized materials and (2) the physical and chemical consequences of miniaturization. The technological payoffs range from the development of new and useful types of DNA detection strategies to high-performance catalysts and, perhaps, even to the realization of bioelectronic nanocircuitry.

Advances in nanotechnology will require us to utilize techniques and concepts from almost every area of science and engineering. I want to emphasize that synthetic chemists in general, and inorganic chemists in particular, have much to offer this emerging field. Traditionally, inorganic chemists have been very good at crossing and merging disciplines in order to ask and answer key questions in modern science. As you will see, an appreciation of the techniques, skills, and fundamental concepts used broadly in the fields of chemistry, materials science, physics, and even biochemistry is essential to make the projects that I am going to discuss today successful.

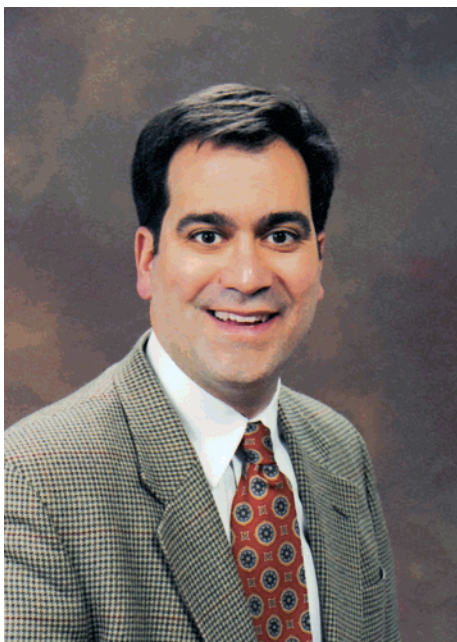
Nanotechnology

Nanotechnology is a field aimed at fabricating, studying, manipulating, and exploiting the properties of structures with dimensions on the nanometer length scale. Prior to the invention of the scanning tunneling microscope, nanotechnology was a topic primarily discussed by science fiction writers rather than conventional scientists. Scanning probe instruments, which enable one to easily manipulate structures on the nanometer, or even angstrom, length scale, combined with synthetic advances over the last century for preparing nanometer-sized objects and quantum-confined materials, have paved the way for the transitioning of nanotechnology from science fiction to a meaningful scientific endeavor.

There are three main challenges in the field of nanotechnology. The first is to develop a combination of tools and materials that allow us to make small structures and control the architecture of large structures on the nanometer length scale. Of course, we must be able to do this routinely before we can really explore this field in detail. The second important challenge is to determine the chemical and physical consequences of miniaturization. This is where the real science is in nanotechnology. We already know that there can be significant consequences such as the particle-size-dependent emission properties of semiconductor quantum dots (QDs), the unusual ion and electron transport properties of two-dimensional films, and the cooperative chemical reactivity of organized assemblies. As the field evolves we will see many more examples, and later in my presentation, I will talk about one involving the distance-dependent optical properties of gold nanoparticles. Finally, if this field is going to be sustained, we ultimately have to be able to exploit the consequences of miniaturization in developing new and useful types of technology. The two projects that we will discuss here today will touch on all three of these issues.

[†] This article is an edited transcript of the presentation given by Chad A. Mirkin (Northwestern University, Chemistry Department), recipient of the 1999 ACS Award in Pure Chemistry. Date and place given: 217th ACS National Meeting, March 22, 1999, Anaheim, CA. Some recent examples of research advances since the talk have been included.

[‡] Selected references are provided in footnotes 1–7. This list is not meant to be comprehensive but rather a reflection of those given in the presentation.



Chad Mirkin received his B.S. from Dickinson College in 1986 and his Ph.D. in chemistry from The Pennsylvania State University in 1989. In the same year he became an NSF Postdoctoral Fellow at MIT. He joined the faculty of Northwestern University in 1991, and in 1997 he assumed the Charles E. and Emma H. Morrison Professorship of Chemistry. Mirkin currently holds the George B. Rathmann Chair in Chemistry and is Director of the NU Center for Nanofabrication and Molecular Self-Assembly. Mirkin's multidisciplinary research program focuses on the interfaces of organometallic chemistry, surface chemistry, and electrochemistry. His main research interests are (1) surface coordination chemistry and design, (2) sensor development, and (3) the rational design of hybrid ligands for electrochemically controlling transition metal stoichiometric and catalytic reactivity. Mirkin's honors include the ACS Award in Pure Chemistry, the MRS Outstanding Young Investigator Award, the E. Bright Wilson Prize, the Phi Lambda Upsilon Fresenius Award, and the B.F. Goodrich Collegiate Inventors Award. Professor Mirkin is the author or coauthor of over 100 publications and nine patents and is an active consultant with several major chemical companies.

The first project pertains to the development of biological-based methods for directing the assembly of nanoscale inorganic building blocks into functional materials.¹ Specifically, our goal is to learn how to control the nanoscale architecture of extended materials by using DNA as a synthetically programmable assembler. The second project involves the development of a new tool for making molecule-based patterns with sub-100-nm resolution. Here, we have developed a new type of soft lithography that allows one to routinely prepare one-molecule-thick structures with 15-nm line-width resolution. These projects are highly complementary and are leading to a general way of

building and manipulating two- and three-dimensional nanostructured materials.

Biomolecular Building Blocks

In the first area (biomolecular building blocks), we are developing methods for functionalizing small inorganic building blocks with DNA and then using the molecular recognition properties associated with DNA to guide the assembly of those particles or building blocks into extended structures. Our aim is to be able to control the particle chemical composition, the particle size, the distance between the particles, and the strength of the interactions between the particles in the resulting nanostructured materials. Why? If we can do this, we can, in principle, control all the important properties of the resulting structures. The first topic can be illustrated by this analogy: DNA is like a bricklayer responsible for assembling the nanoscale building blocks, and it also acts as the "mortar" holding everything together in the extended architectures we intend to generate; the particles are the bricks or building blocks that impart physical properties into the resulting structure.

Although DNA arguably is the most tailorable and versatile molecule for organizing nanoscale materials into extended structures, it has some limitations. Most notably, it is not a high-temperature material, and, therefore, the structures initially generated from DNA interconnects will not be stable at elevated temperatures. However, I maintain that there are many specialty materials based on this programmed assembly approach that we can generate that can provide significant insight into the science of small structures and also allow us to develop some useful technologies. I will discuss some synthetic methods that we have developed over the past couple of years, some of the structures that we have generated using this type of approach, and some of the unique properties associated with those structures. I also want to tell you about one application in particular that pertains to a new type of DNA diagnostic method, which is based upon some nanostructured materials generated via our DNA-driven materials synthesis strategy.

For our synthetic method to work, we need both nanoparticle and DNA-based building blocks. The good news is that we have many nanoparticle building blocks already available to us (Table 1).²⁻⁴ We have metals, semiconductors, magnetic particles, and polymer particles. The sizes of these particles can be controlled in many cases from 1 nm to 1 μm in diameter. Although the syntheses of such particles all have not yet been perfected, we do have a very good starting point. We are at the stage in the development of this field where particle assembly and synthesis methods need to be developed in concert if we are going to make full use of these nanoparticle materials.

For this presentation, I will focus on one particular type of particle, based upon gold. However, keep in mind that we have

(1) Mirkin, C. A.; Letsinger, R. L.; Mucic, R. C.; Storhoff, J. J. A DNA-Based Method for Rationally Assembling Nanoparticles into Macroscopic Materials. *Nature* **1996**, *382*, 607–609. (b) Elghanian, R.; Storhoff, J. J.; Mucic, R. C.; Letsinger, R. L.; Mirkin, C. A. Selective Colorimetric Detections of Polynucleotides Based on the Distance Dependent Optical Properties of Gold Nanoparticles. *Science* **1997**, *277*, 1078–1081. (c) Storhoff, J. J.; Elghanian, R.; Mucic, R. C.; Mirkin, C. A.; Letsinger, R. L. One-Pot Colorimetric Differentiation of Polynucleotides with Single Base Imperfections Using Gold Nanoparticle Probes. *J. Am. Chem. Soc.* **1998**, *120*, 1959–1964. (d) Mucic, R. C.; Storhoff, J. J.; Mirkin, C. A.; Letsinger, R. L. DNA-Directed Synthesis of Binary Nanoparticle Network Materials. *J. Am. Chem. Soc.* **1998**, *120*, 12674–12675. (e) Mitchell, G. P.; Mirkin, C. A.; Letsinger, R. L. *J. Am. Chem. Soc.*, in press. For reviews, see: (f) Storhoff, J. J.; Mucic, R. C.; Mirkin, C. A. *J. Cluster Sci.* **1997**. (g) Storhoff, J. J.; Mirkin, C. A. *Chem. Rev.* **1999**, *99*, 1849–1862.

(2) Hayat, M. A. *Colloidal Gold: Principles, Methods, and Applications*; Academic Press: San Diego, 1991. (b) Creighton, J. A.; Blatchford, C. G.; Albrecht, M. G. *J. Chem. Soc., Faraday Trans. 2* **1979**, *75*, 790–798. (c) Henglein, A.; Ershov, B. G.; Malow, M. *J. Phys. Chem.* **1995**, *99*, 14129–14136. (d) Curtis, A. C.; Duff, D. G.; Edwards, P. P.; Jefferson, D. A.; Johnson, B. F. G.; Kirkland, A. I.; Wallace, A. S. *Angew. Chem., Int. Ed. Engl.* **1988**, *27*, 1530–1533.

(3) Murray, C. B.; Norris, D. J.; Bawendi, M. G. *J. Am. Chem. Soc.* **1993**, *115*, 8706–8715. (b) Chestoy, N.; Hull, R.; Brus, L. E. *J. Chem. Phys.* **1986**, *85*, 2237–2242. (c) Wang, Y.; Herron, N. *J. Phys. Chem.* **1991**, *95*, 525–532. (d) Kavan, L.; Gratzel, M.; Rathousky, J.; Zukal, A. *J. Electrochem. Soc.* **1996**, *143*, 394–400. (e) Spanhel, L.; Anderson, M. A. *J. Am. Chem. Soc.* **1991**, *113*, 2826–2833. (f) Heath, J. R.; Williams, R. S.; Shiang, J. J.; Wind, S. J.; Chu, J.; D'Emic, C.; Chen, W.; Stanis, C. L.; Bucchignano, J. J. *J. Phys. Chem.* **1996**, *100*, 3144–3149.

(4) Feltin, N.; Pileni, M. P. *Langmuir* **1997**, *13*, 3927–3933.

Table 1. Representative Nanoparticle Compositions and Sizes

particle composition	available particle size (nm)
metals ²	
Au ^A	2–150
Ag ^B	1–80
Pt ^C	1–20
Cu ^D	1–50
semiconductors ³	
CdX (X = S, Se, Te) ^A	1–20
ZnX (X = S, Se, Te) ^B	1–20
PbS ^C	2–18
TiO ₂ ^D	3–50
ZnO ^E	1–30
GaAs, InP ^F	1–15
Ge ^G	6–30
magnetic ⁴	
Fe ₃ O ₄	6–40
polymer	
many compositions	50–1000

developed surface modification methods for cadmium selenide, cadmium sulfide, and a variety of other magnetic and polymer compositions. The particle assembly methods that I describe are completely general as long as one can immobilize synthetic DNA onto nanoparticle surfaces. This is not trivial and often requires a detailed understanding of the surface coordination chemistry of the particles of interest so that nonspecific interactions between two types of DNA-labeled particles can be eliminated. In our scheme, the particles provide the physical properties, but the DNA does all of the chemical assembly work.

Why did we choose gold? First, gold nanoparticles can be made with two commercially available starting materials, hydrogen tetrachloroaurate and sodium citrate (Figure 1A). These two reagents are simply combined in a reaction vessel on a benchtop, and by adjusting the stoichiometric ratio of the reagents, the sizes of the resulting particles can be controlled. In this experiment, we were trying to prepare 13-nm particles. Note that this method was developed by Frens et al.,^{5a} and later improved by Natan,^{5b} but the scientific study of such particles extends back to Michael Faraday in the late 1800s. In addition to the nanoparticles, the preparatory procedure also leads to a variety of organic and inorganic byproducts (Figure 1A). How do we know we have 13-nm particles? Looking at the UV–vis spectrum of the solutions containing the particles (Figure 1B), we see the characteristic plasmon band at 520 nm. The breadth and position of the plasmon band are related, to some extent, to the average size and polydispersity of the particles. On the basis of the spectroscopic data, one can conclude that this is a fairly monodisperse sample. Figure 1C shows the TEM image of the solution, which confirms the presence of the gold nanodots. Some are slightly irregular in shape, which is, in part, an artifact of our TEM experiment. Under certain conditions, the electron beam moves the particles or even causes them to fuse together. However, once they are modified with DNA, they become indefinitely stable.

Nanoparticle Model

It is believed that each particle has a Au⁰ core and a Au^I shell due to incomplete reduction at the nanoparticle surface. Citrate and chloride are coordinated to the Au^I shell. So overall, each particle is net anionically charged. Since the molar extinction coefficient of the plasmon band in the spectrum of the nanoparticles is approximately $2.4 \times 10^8 \text{ M}^{-1} \text{ cm}^{-1}$, solutions of these particles are highly colored. For benchmarking

purposes, these particles are more intensely colored than phthalocyanine dyes. This will become a significant asset with regard to some of the applications I will discuss later in my talk, in particular, ones involving diagnostic methods.

How do we know such particles are charged? There is a wonderful general chemistry experiment one can do to demonstrate their charged nature. The addition of an electrolyte to a solution containing the particles will result in a decrease in interparticle distance, due to charge screening effects. This decrease in interparticle distance results in a concomitant red shift in the particle plasmon band. Therefore, when salt is added to a solution of 13-nm particles, the particles aggregate and the solution color turns from red to blue, Figure 2. This not only is a nice demonstration of the charged nature of the particles but also shows how one can manipulate their optical properties. For background regarding the development of the surface coordination chemistry of the particles, I refer readers to the literature.¹

The paper that initiated much excitement about the prospect of using DNA in conjunction with inorganic materials in nanostructure assembly,^{1a} and in a way initiated a new field, was done collaboratively with my colleague, Emeritus Professor Robert Letsinger. Over the past few years, we have been working very closely together on the development of materials assembly methods based on DNA-modified nanoparticles. The initial strategy that we adopted is shown in Scheme 1. In this work, two batches of gold nanoparticles were prepared, and each was functionalized with noncomplementary single-stranded DNA. An attractive aspect of using DNA as an interconnect molecule is that, with a synthesizer, one can prepare just about any sequence one desires. DNA can be prepared and functionalized with virtually any chromophore, acceptor, donor, or redox-active group in automated fashion. In addition, particle-binding functional groups can be easily attached to such sequences. One also can prepare DNA-based interconnect molecules that span larger distances than conventional organic molecules. For example, it is trivial to make a 200-Å-long oligonucleotide in pure form in about an afternoon, and although it is conceivable that one could prepare an organic interconnect molecule of similar length, it likely would take a long time to synthesize and isolate the compound. Finally, with DNA, one can program into the system rationally triggerable recognition events based upon the simple base-pairing schemes associated with DNA.

The idea, then, was to synthesize two different sequences of DNA that have alkanethiol end-groups and immobilize them on two batches of 13-nm particles, respectively, Scheme 1. How many oligonucleotides are on each 13-nm particle? Through fluorescent labeling studies, we have determined this to be, on average, about 220 oligonucleotides. Not all of these strands are capable of hybridization. Remember that hybridization is the process of bringing two single-stranded DNA molecules together to form duplex DNA. At this loading level, only about 15% of the strands are available for hybridization. The tradeoff here is that we have to load the particles with oligonucleotides to the point that they are stable in aqueous media at moderate salt concentrations, but not to the point where there will not be enough room to bring in linking strands. Particle stability is a significant issue, especially since DNA and the conditions used to effect hybridization are naturally incompatible with many nanoparticle compositions. As I showed earlier in this presentation, salt causes most charge-stabilized nanoparticles to aggregate irreversibly. This is especially true in the case of gold nanoparticles. Therefore, we had to develop methods that allowed us to slowly load up the oligonucleotides on the particle

(5) (a) Frens, G. *Nature Phys. Sci.* **1973**, *241*, 20–22. (b) Grabar, K. C.; Freeman, R. G.; Hommer, M. B.; Natan, M. J. *J. Anal. Chem.* **1995**, *67*, 735–743.

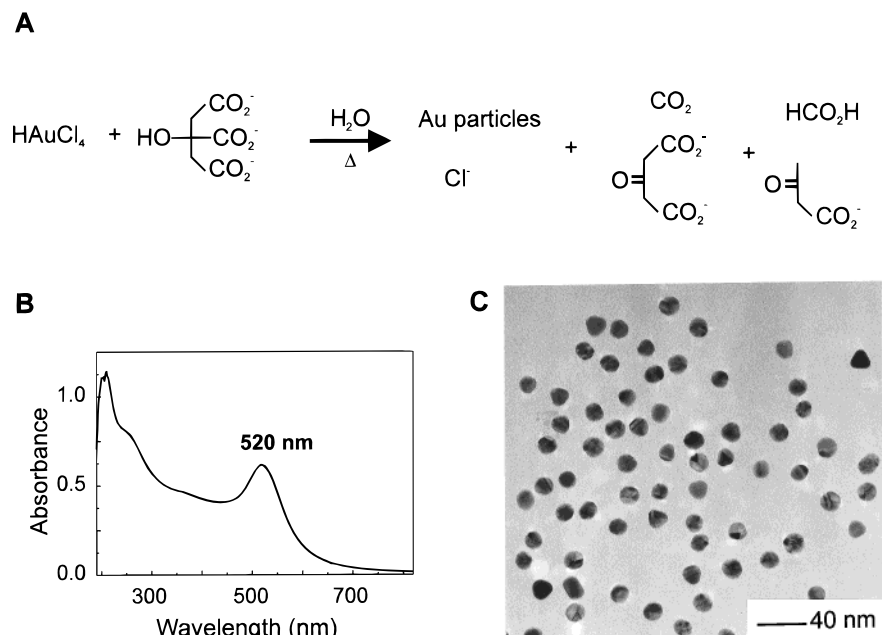


Figure 1. (A) Synthetic method for preparing 13-nm Au particles. (B) UV-vis spectrum of an aqueous solution of 13-nm particles. (C) TEM image of 13-nm gold particles cast onto a holey carbon grid.

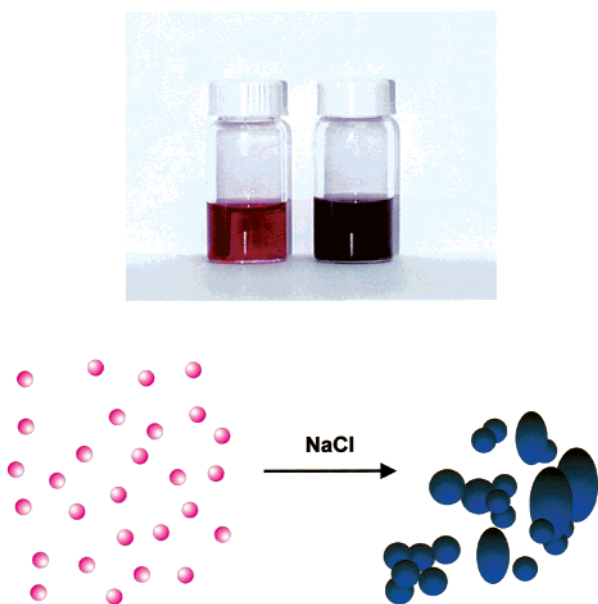
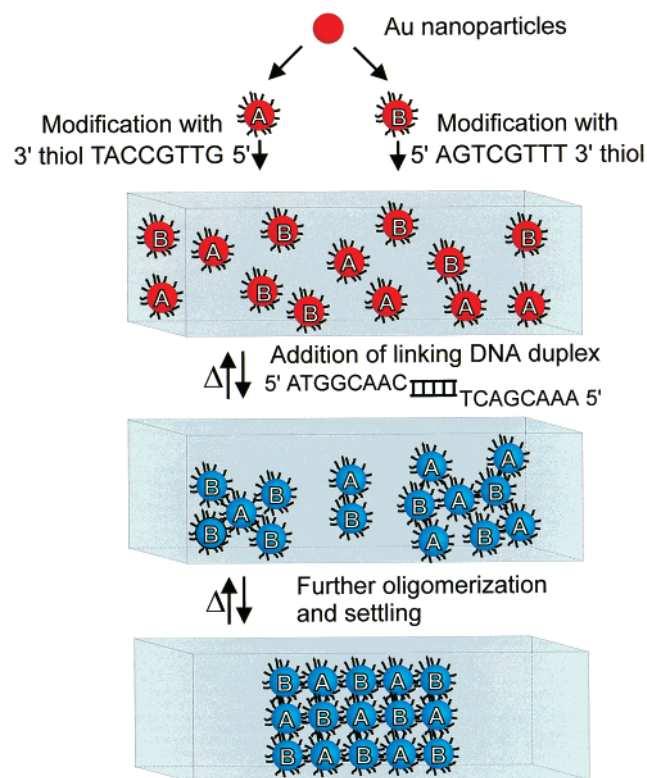


Figure 2. Aqueous solution of 13-nm-diameter Au particles before (red) and after (blue) the addition of NaCl. This is an irreversible process.

surface without effecting irreversible and nonspecific particle aggregation.

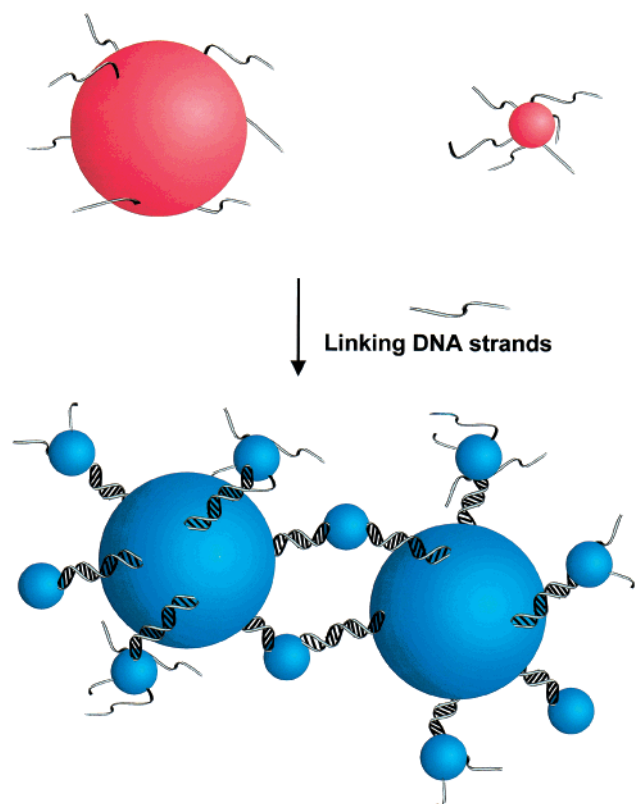
In our initial experiments, we designed two noncomplementary oligonucleotide sequences that could be immobilized on the surfaces of two sets of gold nanoparticles. When we mix these two batches of particles, they do not recognize one another and, therefore, look like a dispersed set of particles and are red in color (Scheme 1). If we want to induce an assembly event, we add a linking oligonucleotide strand. In this case it is duplex DNA with a 12-base-pair overlap in the middle. The interior duplex portion of this linking strand is not so important. The key here is that there are floppy ends on the linker DNA which perfectly recognize the sequences immobilized on the two different batches of gold nanoparticles. Once we add the linker to the solution, the particles begin to come together. As they

Scheme 1



assemble, we see a red shift in the plasmon band, which correlates to a red-to-blue color change as detected by the naked eye. We can drive this system to an extended macroscopic structure by annealing it and allowing large aggregates to grow. The molecular recognition properties of the DNA dictate that the particles in the final structure will assume an AB-AB periodicity. This must be the case if the molecular recognition properties of the DNA, and not nonspecific interactions, are driving this assembly process. Remember that hybridization is a reversible process, so if the method results in a nonthermodynamic structure, the DNA interconnects can be broken by

Scheme 2



heating, and the system can be driven to the thermodynamic structure by reassembling under a different set of conditions. This is not possible with normal salt-flocculated gold particles. Once such particles aggregate, larger clusters form, eventually resulting in the precipitation of bulk gold.

I vividly recall the first experiment with this system, as it was quite amazing. My students, Robert Mucic and James Storhoff, came running down to my office late one evening and said, "Chad, you've got to take a look at this." They had dispersed particles in one cuvette, and after addition of the DNA linking strand to the cuvette containing the particles, the color of the solution changed to what we now like to call "North-western purple", Figure 3B, cuvette B. As we let the solution stand for about an hour and a half, a polymeric precipitate formed and settled to the bottom of the reaction vessel, Figure 3B, cuvette C. If either cuvette B (DNA-linked particles) or cuvette C (precipitated aggregates of DNA-linked particles) was placed in an oven, the solution color changed back to red (as depicted by cuvette A). When we moved the dissociated system back to the benchtop, it quickly went back to state B. This was done repeatedly with no evidence of particle degradation or agglomeration under such conditions. Figure 3A provides a spectroscopic measure of what was happening: as particles were linked together with DNA, the plasmon band shifted from 520 to approximately 600 nm. It also became much broader, giving rise to the striking red to bluish-purple color changes. It's interesting to note that the extinction at 260 nm also drops significantly as this process takes place. This is primarily due to an aggregate density effect. As these large networks of particles are generated, the sample is effectively diluted, at least with respect to the UV-vis spectroscopy. Essentially, the excitation source does not sample a portion of the interior of the aggregate. The spectroscopic signal continues to decrease in intensity as extended aggregates are generated.

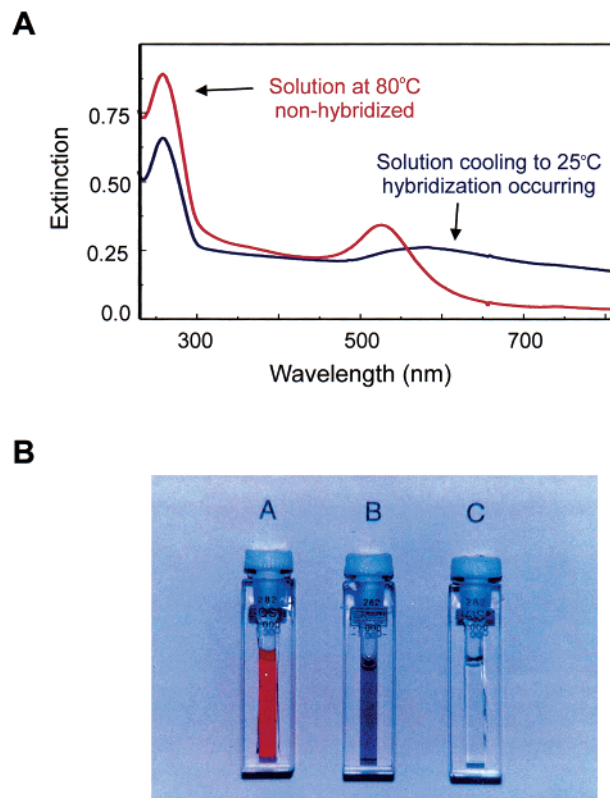


Figure 3. (A) The UV-vis spectrum of oligonucleotide-modified 13-nm particles before (red line) and after (blue line) DNA-induced assembly. (B) Solutions of 13-nm-diameter Au particles before (cuvette A) and after (cuvette B) DNA-induced assembly. After extended periods of time a polymeric precipitate forms and settles to the bottom of the cuvette (cuvette C). (Reproduced with permission from ref 1a. Copyright 1996 Macmillan Publishers Ltd.)

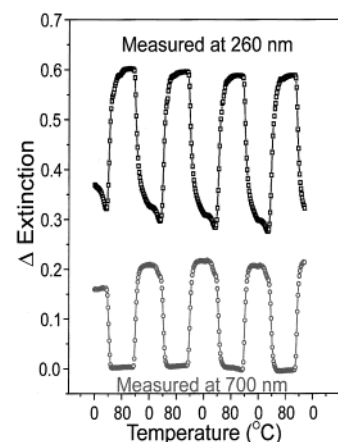


Figure 4. Extinction changes at 260 (squares) and 700 nm (circles) as a function of temperature for DNA-linked particles. (Reproduced with permission from ref 1a. Copyright 1996 Macmillan Publishers Ltd.)

This thermally induced DNA dissociation process is very reversible. Let us examine what occurs if we monitor the process at 260 nm as a function of temperature (Figure 4). This is typically how a DNA chemist would follow this linking or unlinking process, which is often referred to as "melting". For DNA, the extinction at 260 nm is associated with a transition dipole in the bases that is quenched when duplex DNA is formed. As the system is heated, the duplex DNA unravels with a concomitant increase in extinction at 260 nm. With our DNA-linked particles, we observe dips in extinction just prior to the

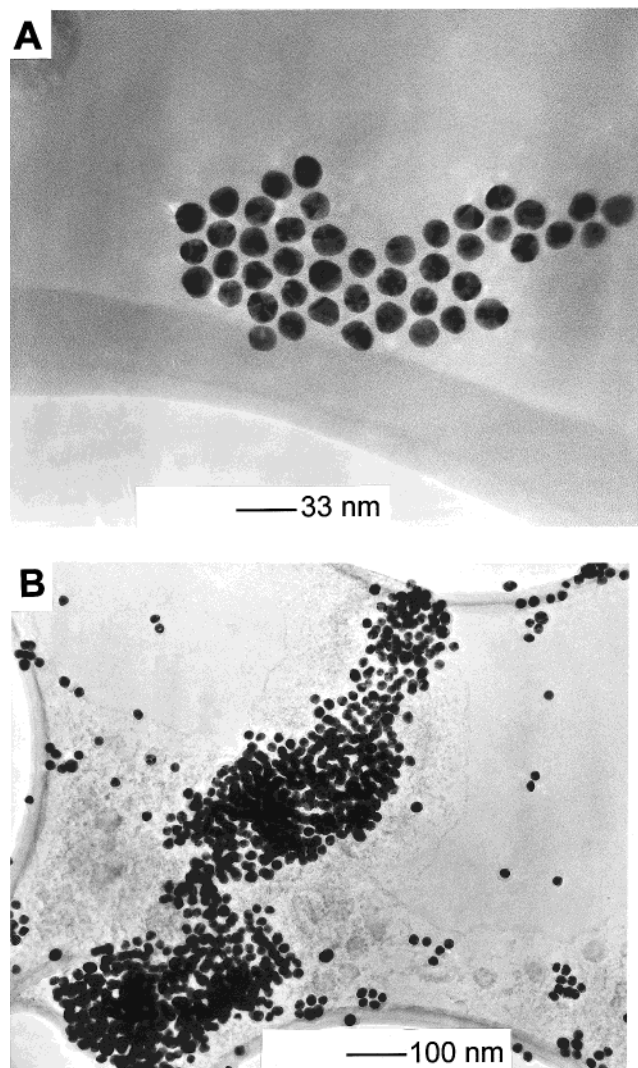


Figure 5. TEM images of DNA-linked nanoparticle assemblies at early stages in the growth process. (Reproduced with permission from ref 1a. Copyright 1996 Macmillan Publishers Ltd.)

melting transition. The system can be cycled repeatedly between room temperature and 80 °C with the change in extinction associated with the melting processes being comparable in magnitude. This is characteristic of a system that is stable over this temperature range.

In our system the signature at 260 nm is due in part to the particles. However, to make absolutely sure that the particles were participating in this assembly process, we monitored a spectroscopic signature at 700 nm, which is clearly due to the particles rather than the DNA. When the particles are aggregated at room temperature, there is a significant extinction increase at 700 nm. As the system is heated above the melting temperature of the DNA, the particles disperse and the extinction at 700 nm drops to zero. We then calculated how much DNA was actually present in solution, and determined what type of extinction change we should see at 260 nm. It turned out that there was not enough DNA in this experiment to account for the magnitude of extinction changes we were observing. Therefore, the extinction change at 260 nm, in the case of the system with nanoparticles, is due primarily to the nanoparticles and not DNA. We have been modeling the optical properties of these particles with Professor George Schatz, one of our resident theoreticians. The modeling studies are completely consistent with our experimental observations, but for the sake

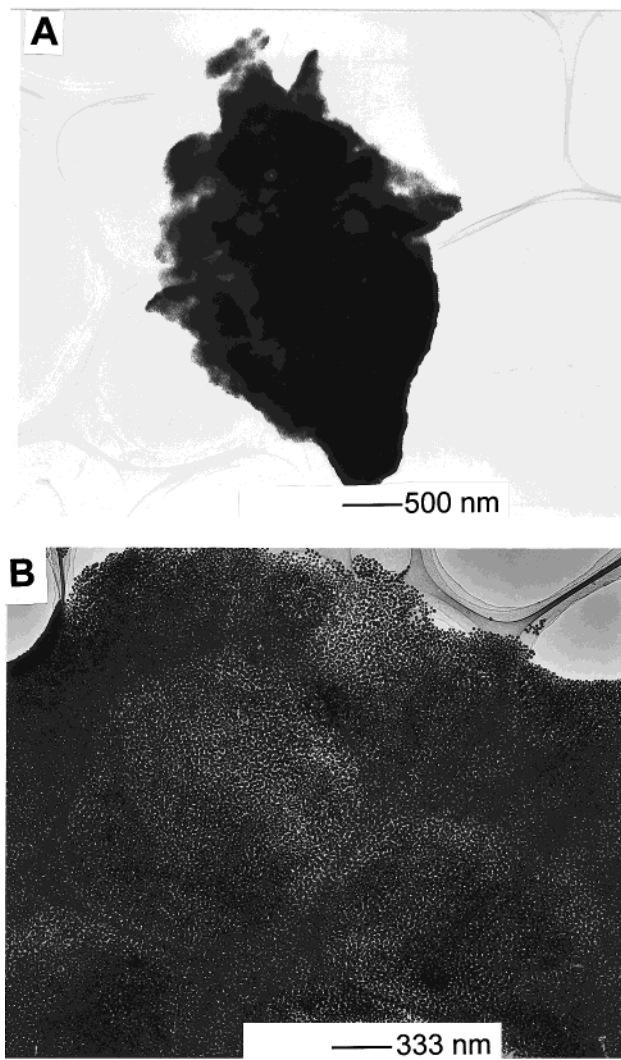


Figure 6. TEM images of annealed assemblies of DNA-linked 13-nm particles.

of brevity, I will not go into the details of those results for this presentation. Interestingly, monitoring the spectroscopic signature at 260 nm associated with the nanoparticles becomes a much more sensitive way of following DNA dehybridization or detecting DNA, since we obtain a melting curve that is a reflection of the DNA interconnects, despite the fact that we are spectroscopically probing the nanoparticles. This has significant implications with respect to studying the DNA-dehybridization process, as much lower detection limits can be achieved by monitoring signatures associated with these probes rather than a spectroscopic signature associated with the bases.

One interesting question is: Why has DNA not been used extensively in materials synthesis until now, and why is there such an intense interest in using it now? I have always said and still maintain today that DNA is the quintessential building block for materials synthesis. The advantage of using DNA as a materials synthon rather than a conventional organic interlink molecule is that it is synthetically programmable and very predictable from a reactivity standpoint. With DNA, most of the structures that we write on the black board can be prepared in the laboratory, provided that we understand the simple base-pairing interactions of DNA. The beauty of working with hybrid inorganic/DNA structures is that we have an enormous characterization-capability advantage over those who work with materials made solely of DNA.

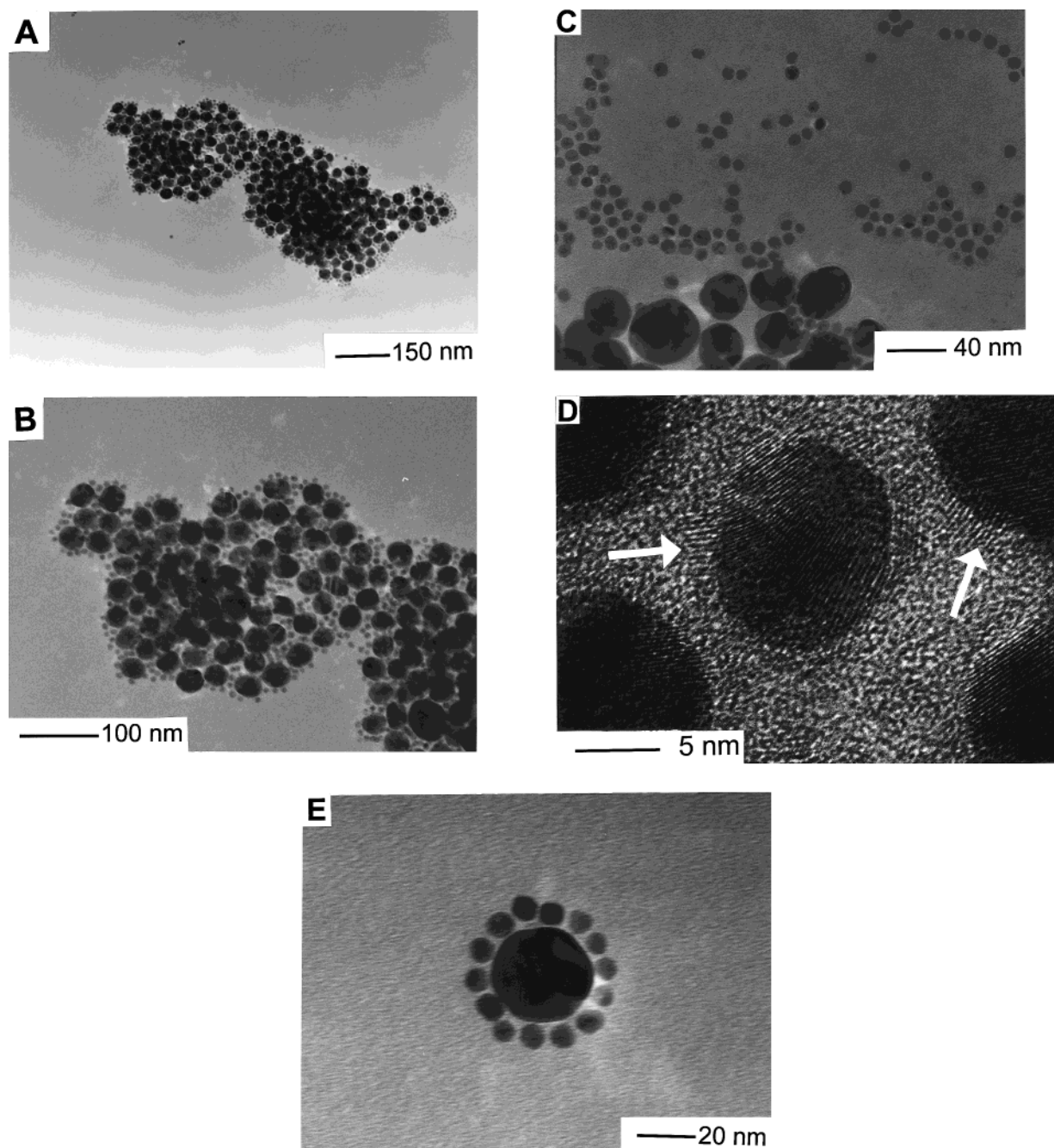
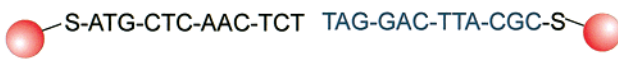


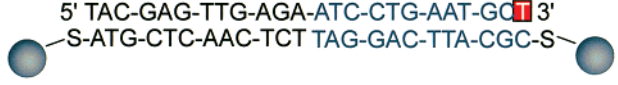

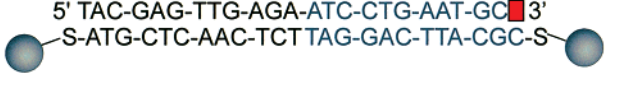
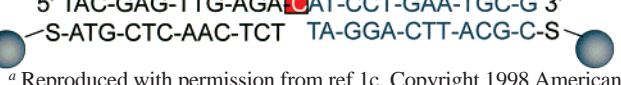


Figure 7. TEM images of binary DNA-linked network materials. (A) An assembly formed from 8- and 30-nm gold particles. (B) A higher resolution image of a portion of the aggregate displayed in panel A. (C) The results of a control experiment involving 8- and 31-nm particles without DNA linker. (D) HR-TEM image of a portion of a hybrid Au/QD assembly. The lattice fringes of the QDs, which resemble fingerprints, appear near each Au nanoparticle. (E) A satellite structure formed by using a 60-fold excess of the 8-nm particles. (Reproduced with permission from ref 1d. Copyright 1998 American Chemical Society.)

When we merge DNA with inorganic building blocks, we can exploit some of the properties of the latter to follow the assembly process and characterize the resulting products. For example, electron microscopy can be used to image assembled networks of particles and gain information about the assembly process (Figure 5A). Early on in the assembly process, we often observe small, two-dimensional particle arrays. The aggregates then grow into larger three-dimensional structures (Figure 5B) and then, eventually, grow into massive aggregate structures that span macroscopic dimensions, Figure 6. On the basis of the melting profiles of these structures, we know that they are linked by DNA. Also note that every particle within these aggregates is still intact and shows no evidence of fusing with

other particles. This demonstrates the second important role that the DNA plays in this process. It is an excellent steric and electrostatic protector of the particles. Therefore, only sequence-specific binding events will drive the particle assembly process. Although one might look at Figure 6A and think of the assembled structures as just a blob of particles, it is substantially more than that. The reason this demonstration is so important is that, by using DNA, we have assembled many millions of nanoparticles into structures that have dimensions typically associated with physical deposition techniques. One can view this as a biologically inspired, bottom-up approach to materials synthesis. The tailorability of this system with respect to the types of structures that we can generate is virtually limitless,

Table 2. DNA-Modified Nanoparticle Probes and Targets Used for the Selectivity Studies^a

A Probes with No Target	
B Half-Complementary Target	5' TAC-GAG-TTG-AGA- GAG-TGC-CCA-CAT 3' 
C Complementary Target	5' TAC-GAG-TTG-AGA-ATC-CTG-AAT-GCG 3' 
D One Base-Pair Mismatch at Probe Head	5' TAC-GAG-TTG-AGA-ATC-CTG-AAT-GC T 3' 
E One Base-Pair Mismatch at Probe Tail	5' TAC-GAG-TTG-AGA- CTC -CTG-AAT-GCG 3' 
F One Base Deletion	5' TAC-GAG-TTG-AGA-ATC-CTG-AAT-GC TT 3' 
G One Base-Pair Insertion	5' TAC-GAG-TTG-AGA- CA T-CCT-GAA-TGC-G 3' 

^a Reproduced with permission from ref 1c. Copyright 1998 American Chemical Society.

and many of these structures are turning out to have very useful properties (*vide infra*).

Still, this demonstration does not reveal anything about our ability to use this methodology to control particle periodicity. To demonstrate this capability, we used two different types of DNA-functionalized particles in the assembly scheme (30-nm and 8-nm particles) (Scheme 2). The idea was to generate network structures with A–B particle periodicity. It is difficult to use electron microscopy to obtain much useful information from large aggregates of structures with such architectural periodicities. Therefore, I provide data on structures formed at intermediate stages during the assembly process, Figure 7A–D. In Figure 7A, we can see that the big particles are surrounded by the small particles. When the image is enlarged (Figure 7B), this periodicity is even more apparent. An interesting question is, what is the actual state of the DNA under the TEM analysis conditions? At present we are not sure, but we suspect that we are getting a snapshot of these structures just after dehybridization. We do know that we never get these types of structures simply by combining aliquots of big and small particles. In fact, they tend to phase segregate as shown in Figure 7c. We also know through solution TEM experiments that dehybridization does take place after prolonged irradiation with the electron beam. Finally, one can form periodic structures from DNA-functionalized particles, which differ in chemical composition. Recently, we were able to extend this methodology to ZnS coated CdSe quantum dots as shown in Figure 7D. This

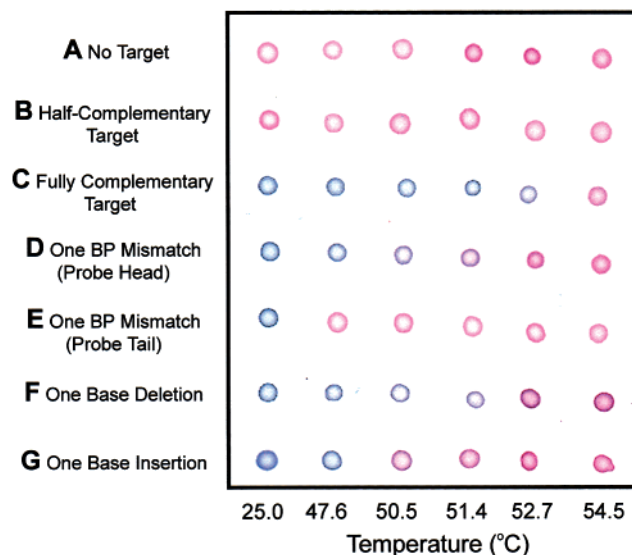


Figure 8. A developed plate showing the ultrahigh selectivity of the “Northwestern spot” method for polynucleotide detection. Sequence information is given in Table 2. (Reproduced with permission from ref 1c. Copyright 1998 American Chemical Society.)

demonstrates the generality and versatility of our approach to materials synthesis.

Interestingly, a new type of nanostructure can be prepared simply by adjusting the ratio of small to big particles. For example, a heavy excess of small particles results in what we refer to as “satellite structures”, in which one big particle is completely surrounded by small particles, Figure 7E. These satellite structures can be separated from excess small particles by centrifugation. Since satellite structures are living polymers, with single-stranded DNA coming off of all of the small particles surrounding the large particles, they form a new type of building block that can be introduced into our assembly scheme to prepare ternary, rather than binary, structures. This process can be extended to form tertiary structures and so on.

So what can we do with this methodology and these novel bioinorganic materials? When we saw the striking colorimetric change associated with the DNA-induced assembly of the 13-nm particles, it became immediately apparent to us that this was a fundamentally new way of following DNA hybridization. Moreover, we suspected that we might have a way of detecting DNA based on a very simple binary (blue/red) color scheme. To determine if these network materials could be utilized to develop a useful detection scheme for DNA, we set out to evaluate the target sensitivity and selectivity of the system. We discovered that the target sensitivity is adequate to do DNA detection in conjunction with polymerase chain reaction (PCR), a method used to amplify the amount of a given target. The primary reason we can do colorimetric detection of DNA with these nanoparticle-based probes at target concentrations where colorimetric organic probes would fail is related to the enormous molar extinction coefficient associated with the nanoparticle plasmon band. A 13-nm particle has a $2.4 \times 10^8 \text{ M}^{-1} \text{ cm}^{-1}$ extinction coefficient, which is 3 orders of magnitude larger than the extinction coefficients of the best organic dye molecules. This allows us to use these particles in detection schemes for DNA at nanomolar target levels. Almost every diagnostic method is interfaced with some sort of target amplification method, so the requirement of PCR, although not optimum, is not a significant limitation.

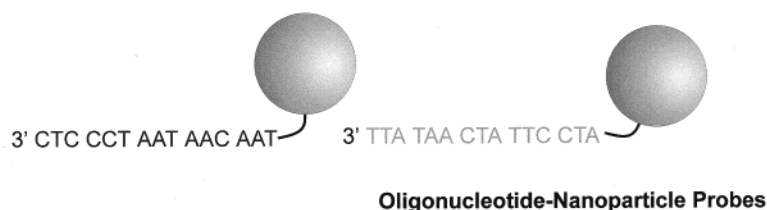
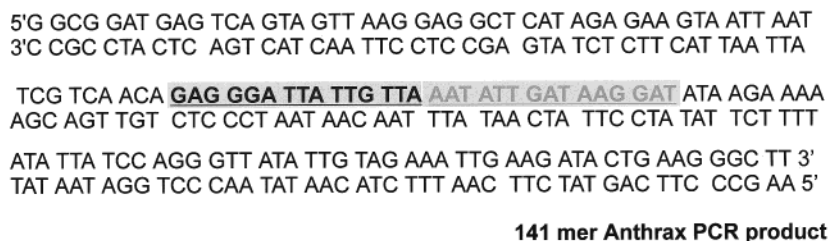


Figure 9. Anthrax PCR product sequence and probe design. The probe recognition sequence is highlighted.

To determine the selectivity of the system, we synthesized a 24-mer sample target and prepared two complementary DNA-functionalized particle probes. Although we show only two probes and one target molecule (Table 2), keep in mind that a network structure consisting of many particles cross-linked with target is formed in all experiments. To evaluate the selectivity of the system, we performed a series of control experiments. Table 2 shows systems with (A) no target; (B) a half-complementary target; (C) a fully complementary target; (D) a target which has a single mismatch on the target end, (E) a single mismatch at the probe tail, (F) a one-base deletion on the end of the target, and (G) a strand with a one-base insertion. Any of the strands of DNA with single-base imperfections could lead to a false positive. In fact, if any of them are added to a solution containing the two particle probes at room temperature, the solution will turn blue since stable duplex DNA structures are formed between these strands and the nanoparticles at room temperature.

However, the imperfect strands can be differentiated from the target by monitoring color as a function of temperature. Think of the hydrogen bonding between the base pairs within the duplex DNA as the glue that holds the structure together. Imperfections, added to the system in the form of mismatches, deletions, or even insertions, will decrease the strength of the interactions holding the duplex DNA together. This will decrease the temperature at which particles interconnected with the DNA come apart and, therefore, the temperature associated with the blue-to-red color change.

As it turns out, there is a very simple way of monitoring the melting process involving these DNA-linked, network nanoparticle-based materials. It simply involves taking a microdroplet of the solution containing the nanoparticles and target and spotting it on a reverse-phase silica gel plate as a function of solution temperature, Figure 8. If the particles are dehybridized and dispersed in solution, when they hit the plate, they form a red spot. If they are hybridized with a target and assembled in solution, they form a blue spot when they hit the plate. Recall that, in solution, the target and probes will rehybridize and turn blue as the system is cooled below the melting temperature of the DNA interconnects. This does not happen on the plate because there apparently is not enough particle mobility to allow for rehybridization. The net payoff is that this spotting provides a permanent record of the detection process. Red spots are observed at every temperature in the 25–54.5 °C range for the two control experiments involving no target or a target that is

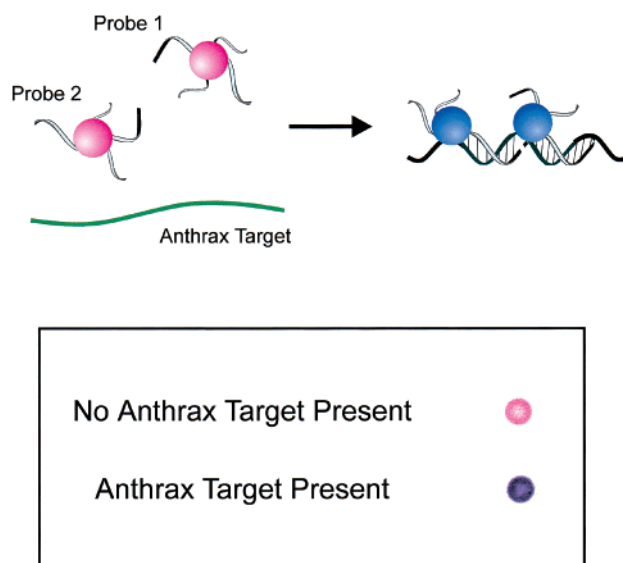


Figure 10. The results of a spot test for solutions with (blue) and without (red) anthrax PCR product.

complementary to only one probe, Figure 8. Keep in mind that we are controlling the temperature of the solution, rather than the plate temperature. Notice that a blue spot forms for the fully complementary target up to 52.7 °C, but at 54.5 °C we see a red spot. All other strands show a red spot at 52.7 °C. This demonstrates that this spot test, based on these nanostructured materials, can be used to differentiate oligonucleotides with very minor imperfections from a perfect 24-nucleotide target. An interesting aspect of this test is that it can be used to differentiate not only the imperfect strands from the perfect target but also the imperfect strands from each other. Indeed, they all have colorimetric transitions at different temperatures.

Thus far, I have discussed DNA detection with these nanoparticle-based materials as it applies to the academic world. What about the real world? In the real world, real targets are used, and they often come in complex environments. A nice aspect of DNA detection is that as long as sequence information is available, particles can be designed to recognize DNA characteristic of any viral, bacterial, or genetic disease. In the case of the biological warfare agent, anthrax, we designed probes that would bind to an interior position of a 141-mer PCR product, Figure 9. This was a big challenge, since we were targeting duplex DNA rather than single-stranded DNA, and a

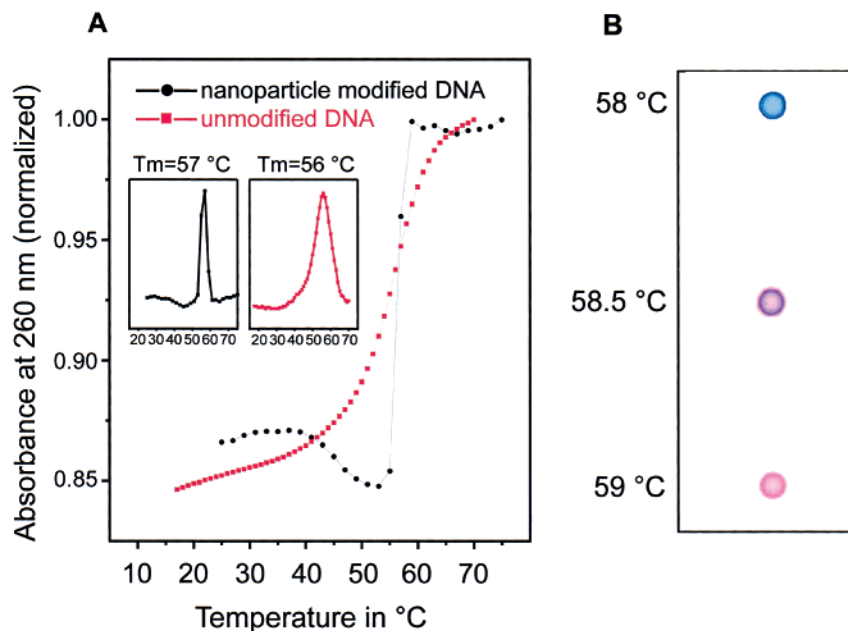


Figure 11. (A) A comparison of the melting transitions for a 30-mer duplex (squares) and nanoparticles linked with the same 30-mer duplex (circles). Absorbance changes are measured at 260 nm. (B) Melting transition for the nanoparticle system as measured by the Northwestern spot test. (Reproduced with permission from ref 1b. Copyright 1997 American Association for the Advancement of Science.)

much larger sequence. In order to detect the anthrax DNA, it is denatured at elevated temperature, and then the appropriate nanoparticle probes are added to the solution containing it. It turns out that the probes, because they have shorter oligonucleotide strands than the complementary target, kinetically win in the rehybridization process. Blockers also were added to the solution to inhibit the target from rehybridizing with its complementary strand. Figure 10 shows the result of the test and a control experiment involving probes but no target: a red spot is observed for the control experiment, and a blue spot is observed for the experiment where anthrax target was present.

I want to stress that this is a very simple DNA detection method, with tremendous selectivity for targeting disease agents, and one which can be interfaced easily with PCR. We have developed another prototype test for tuberculosis and are working on yet another for detecting a gene linked to colon cancer. These are very exciting developments, which underscore the importance of basic research and how it can be transitioned into useful technology. Indeed, all of these detection advances came out of fundamental research aimed at evaluating the properties of DNA as a scaffolding material. This entire project was essentially a “Friday afternoon experiment” when we first started, but it has turned into a major research effort in the group that will continue for many years, perhaps decades.

The real scientific issue, though, is why should this system exhibit higher selectivity than any other diagnostic method based on DNA hybridization? The answer comes from a comparison of melting analyses. Figure 11A shows DNA melting analyses for a system with (circles) and without (squares) nanoparticles. For the system without nanoparticles, one can see the typical broad sigmoidal curve associated with the melting of a short DNA duplex. The system with particles interlinked with the same duplex sequence exhibits a much sharper transition. A big difference between these two melting profiles is that, in the one case, we are focusing on a nanoparticle signature rather than a signature associated with the DNA. With the colorimetric solid-state assay, we also are focusing on a nanoparticle signature rather than a DNA signature, Figure 11B. The

colorimetric melting transition on the plate is striking. At 58 °C the system gives a blue spot; at 58.5 °C the spot is purple; and at 59 °C it is red. The same sequences without particles melt over almost a 30 °C temperature range, Figure 11A (circles). The beauty of the solid-state spot test is that any imperfection that results in a greater than 1 °C destabilization of the duplex-interconnected nanoparticle network can be differentiated colorimetrically from target. Three key factors contribute to the sharp melting profiles associated with the nanoparticle systems: (1) cooperativity due to multiple DNA interconnects in the context of a network structure, (2) the use of a two-particle probe system with distance-dependent and aggregate-size dependent optical properties rather than a single probe or a signature inherent to the DNA, and (3) in the case of the solid-state assay, a solid-state effect, which seems to push the system toward the blue if a critical amount of DNA interlinking has taken place or toward the red if it has not. From a diagnostic standpoint, this sharp melting translates into systems with inherently higher selectivities than conventional single-probe assays.

Dip-Pen Nanolithography

Another related area of research in our group focuses on the development of a new tool for making molecule-based patterns with sub-100-nm resolution. This is a type of soft lithography that we have termed dip-pen nanolithography (DPN).⁶ “Soft” here refers to the chemical composition of the nanostructures we are fabricating. They are made of organic ligands rather than solid-state materials. The work I am going to discuss today is unlikely to displace conventional solid-state fabrication methods. On the contrary, it is highly complementary. Let me explain. If we can develop soft lithography methods, whereby molecules can be patterned in a controlled fashion on the sub-100-nm

(6) (a) Piner, R. D.; Zhu, J.; Xu, F.; Hong, S.; Mirkin, C. A. Dip-Pen Nanolithography. *Science* **1999**, 283, 661–663. (b) Hong, S.; Zhu, J.; Mirkin, C. A. Multiple Ink Nanolithography: Toward a Multiple-Pen Nano-Plotter. *Science* **1999**, 286, 523–525.

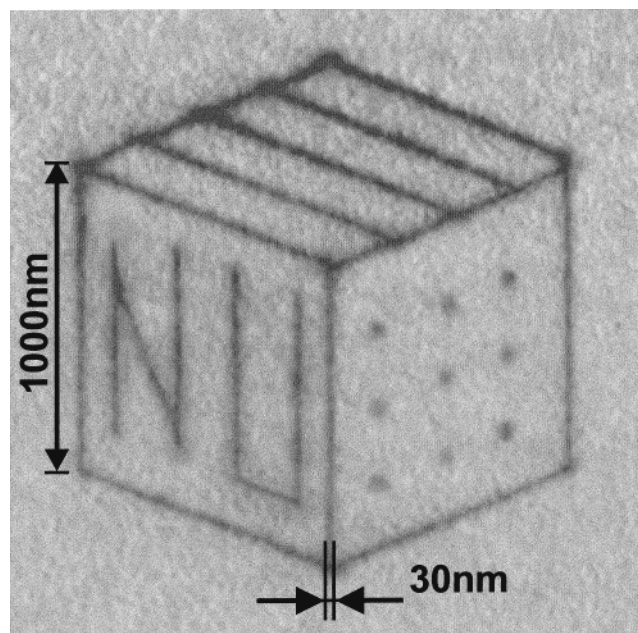


Figure 12. DPN drawing of a cube on Au(111). Each line is made of a monolayer of octadecanethiol.

length scale, many interesting scientific issues pertaining to miniaturization can be addressed. Progress in the field of nanoscale molecule-based electronics has been hampered by the lack of a user-friendly method for generating and aligning nanoscale molecule-based structures between microscopic, macroscopically addressable electrodes, prepared via conventional microfabrication methods. Figure 12 shows one type of structure, which is simply a drawing of a cube, consisting of 1-molecule-thick lines, generated in a chemistry laboratory in a few minutes under ambient conditions. This, of course, would be very difficult, if not impossible, to generate with conventional lithographic methods. Today, I am going to tell you about DPN, a tool we have developed for making such structures, in a matter of minutes, using conventional instrumentation and inorganic surface coordination chemistry.

Dip-pen nanolithography is based upon an atomic force microscope. Unlike many other scanning probe-based lithographic techniques, DPN works under ambient conditions, is a direct-write method, does not require resist layers, and is remarkably routine to use. It, therefore, has the potential to become quite useful. In inventing DPN, the idea was to miniaturize a 4000-year-old technology: the technology of the quill or dip-pen. The big difference was that we wanted to do on a nanoscopic scale what a quill pen can do on a macroscopic scale. Initially, the idea was to cast an ink onto a commercially available AFM tip and transport it to the surface via capillary action. However, this is difficult to control with normal types of molecules and transport solvents. The next step was to design a system with an ink that would chemically react with a substrate of interest, Figure 13. The idea here was that chemisorption could act as a driving force for moving the molecules from the tip to the substrate. However, this was not the only issue that we needed to address. About a year ago, we showed that in any AFM experiment, conducted in air, when the tip comes into contact with the surface, water naturally condenses between the tip and substrate. This is called the "capillary effect". The idea of the capillary effect was not ours and was proposed by many to impede the operation of the AFM in air. Our contribution was showing that the water-filled capillary moves

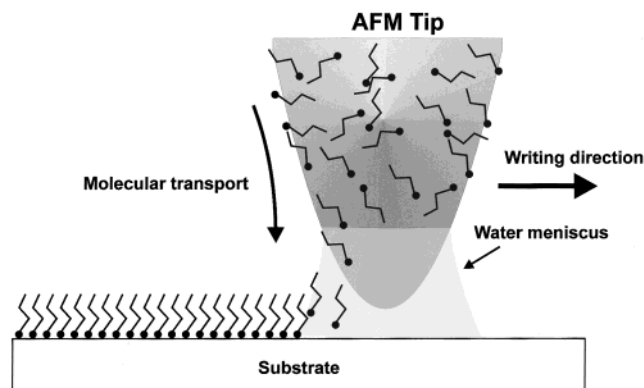


Figure 13. The concept behind DPN. (Reproduced with permission from ref 6. Copyright 1999 American Association for the Advancement of Science.)

with the tip, transporting water as the tip is scanned across a substrate. In air, this cannot be avoided. A postdoctoral associate, Richard Piner, showed that using this concept one can even generate metastable water adlayer structures on a surface.⁷ Generally, metastable structures of water on a surface do not do much for you from a lithography standpoint, but I suggested to Richard that we try to transport molecules that can react with the substrate to form stable 1-molecule-thick nanostructures. The gold-alkanethiol system seemed like a good starting point. The way we ultimately accomplished this was to choose organic molecules with low water solubilities so that the chemisorption driving force would allow us to control the tip-to-substrate transport properties. This would prevent the uncontrolled, nonspecific adsorption and accumulation of multilayers of molecules on the surface. We also found that we could control the effective tip-substrate contact area by controlling the size of the meniscus. Figure 14A shows one example of DPN. Here, we painted octadecanethiol on a $1\ \mu\text{m} \times 1\ \mu\text{m}$ area on an amorphous gold substrate. To be certain that the patterned area consisted of octadecanethiol, we repeated the experiment on a gold(111) substrate. With this atomically flat substrate, it was possible to obtain a lattice-resolved image of the transported self-assembled monolayer of octadecanethiol. The lattice is hexagonal with an intermolecular spacing of $5\ \text{\AA}$, the known lattice constant for an octadecanethiol SAM on gold. The Fourier transform of the data is shown in the lower right hand corner of Figure 14B.

We examined the fundamental properties of this nanopen and discovered that, in some respects, it works much like a normal pen in the sense that ink diffusion from the tip to substrate controls feature size. Figure 15A shows octadecanethiol transported to gold, measured at 2, 4, and 16 min. One can see that the diameter of the spot increases in a manner that is proportional to tip-substrate contact time. In this experiment, we were not trying to optimize the rate of transport, and we now can do this in a matter of seconds by adjusting some of the conditions in the experiment. If we do a similar experiment with 16-mercaptohexadecanoic acid, the ink transport process occurs in seconds, rather than minutes, Figure 15B. Here we see white contrast instead of black. This is because the instrument was run in lateral force mode so that we could differentiate areas by differing forces of friction between tip and sample. In the 16-mercaptohexadecanoic acid case (Figure 15B), we obtain a hydrophilic surface, and in the octadecanethiol case (Figure 15A), we get a hydrophobic surface. In our experiments, white

(7) Piner, R. D.; Mirkin, C. A. *Langmuir* **1997**, *13*, 6864.

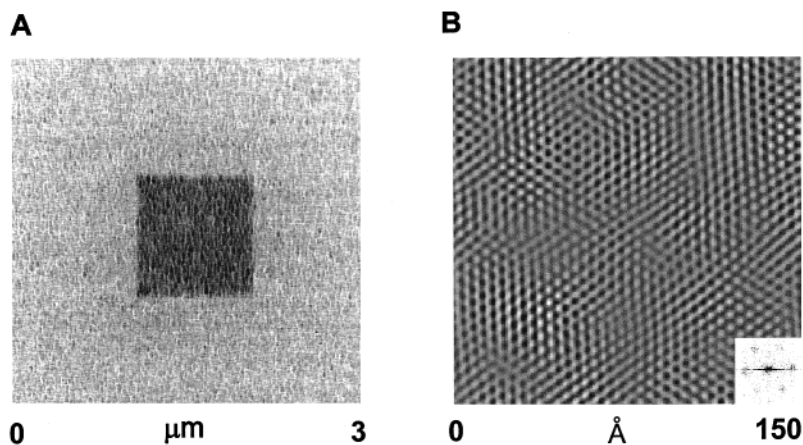


Figure 14. (A) A $1\text{-}\mu\text{m}^2$ SAM of octadecanethiol painted via DPN on gold. (B) Lattice-resolved image of an octadecanethiol nanostructure deposited via DPN on Au(111). (Reproduced with permission from ref 6. Copyright 1999 American Association for the Advancement of Science.)

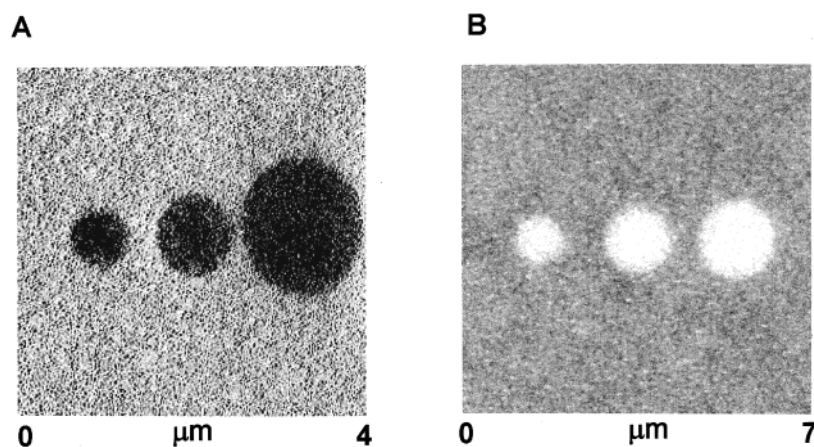


Figure 15. Ink diffusion properties of (A) octadecanethiol at 2, 4, and 16 min (left to right) and (B) 16-mercaptohexadecanoic acid at 10, 20, and 40 s (left to right). (Reproduced with permission from ref 6. Copyright 1999 American Association for the Advancement of Science.)

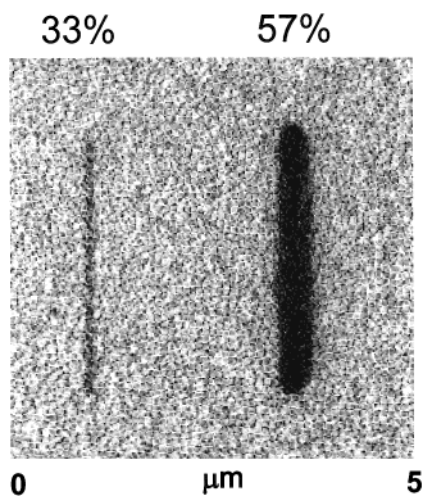


Figure 16. Transport rates of octadecanethiol on amorphous gold as a function of humidity.

always denotes a hydrophilic surface, while black corresponds to a hydrophobic substrate.

Figure 16 shows how humidity allows us to control line width. If one runs the instrument at 33% relative humidity, and then changes it to 57%, one can go from writing 70-nm lines to writing 350-nm lines. In view of the fact that we are controlling humidity with a conventional dehumidifier, this is a remarkably simple way of controlling feature size in a nanolithography experiment.

Types of Structures Generated. Figure 17a shows a molecular grid of octadecanethiol, which is a single molecule thick with 100-nm-wide lines. Note that in this experiment we were not depositing as we imaged. We found that we can control whether or not we are depositing adsorbate by controlling the scan rate. By increasing the scan size, which concomitantly increases scan rate, we essentially do not transport molecules, at least in detectable amounts. Figure 17B shows an array of uniformly deposited 450-nm-diameter dots. Attaining this type of shape regularity and reproducibility would not be possible with a conventional pen, even over macroscopic dimensions. Again, we think the meniscus is responsible for controlling the effective tip–surface contact area and the regular shapes of the features.

Writing with DPN. Letter writing is easily achieved with DPN, as seen in Figure 18A, where we have generated a nanostructure in the form of “AFOSR”. One can see that we have $1\text{-}\mu\text{m}$ features here, with approximately 70-nm line widths. Smaller structures are also possible. In Figure 18B is an example of 60-nm 16-mercaptohexadecanoic acid dots spaced 200 nm apart. The smallest structures that we have prepared thus far are 15-nm-diameter dots spaced 5 nm apart on a gold single crystal substrate, Figure 19.

Multicomponent Nanostructures. Using DPN one can prepare multicomponent nanostructures with near perfect alignment. One can write an initial nanostructure (an array of dots) with octadecanethiol and then write within that initial structure another nanostructure with a different type of ink, Figure 20.

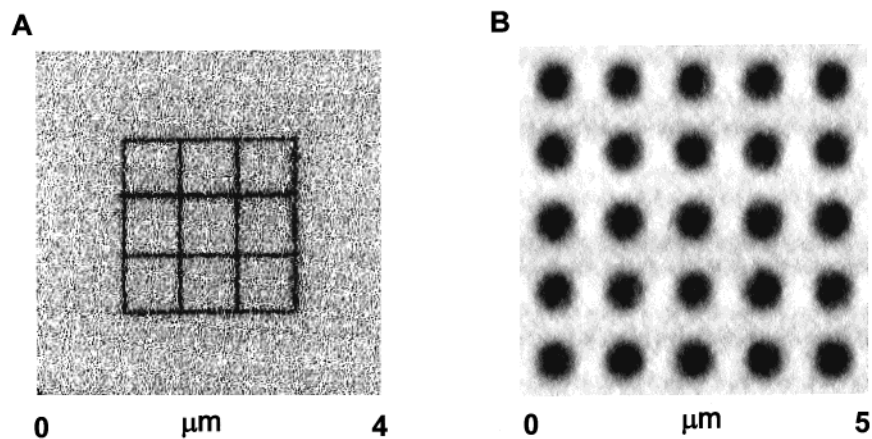


Figure 17. (A) Grid and (B) dot arrays generated via DPN. (Reproduced with permission from ref 6. Copyright 1999 American Association for the Advancement of Science.)

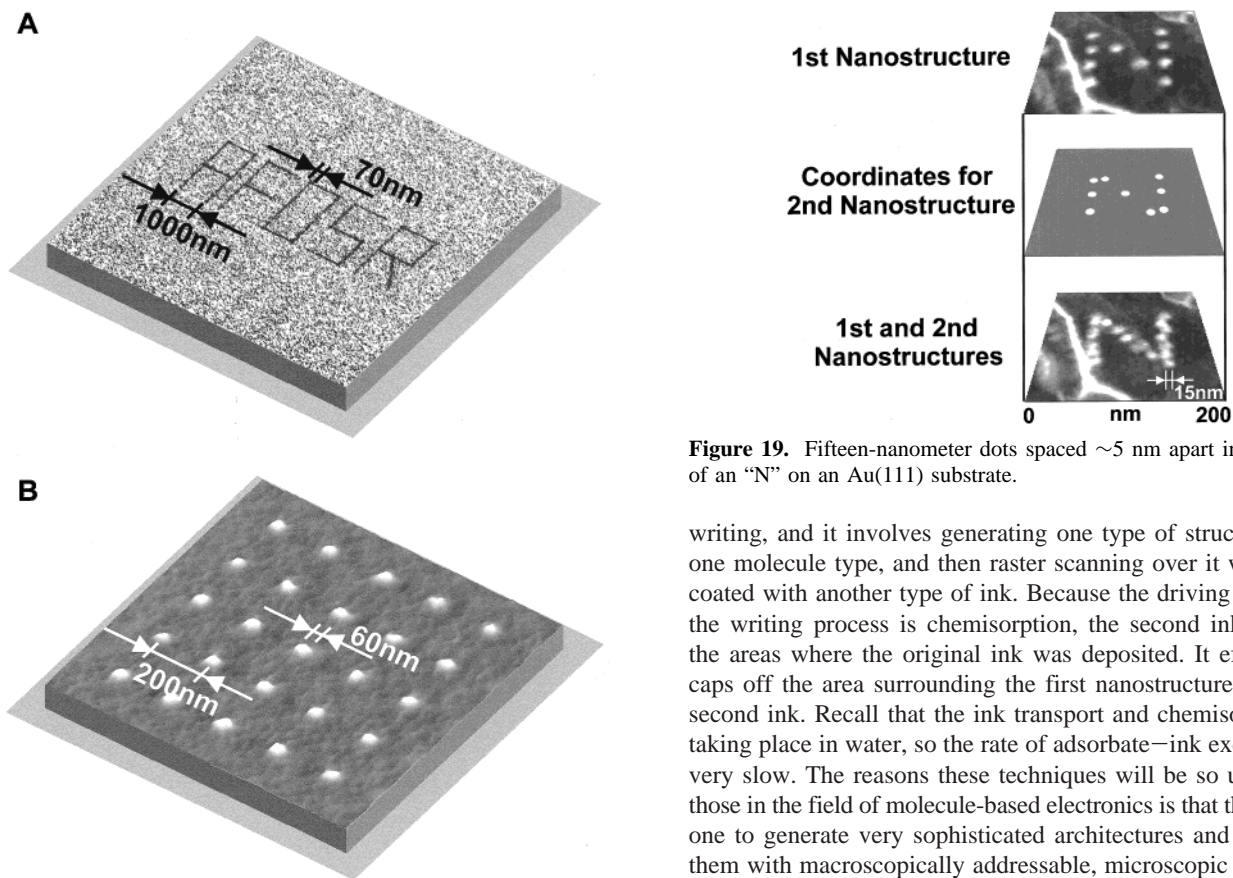


Figure 19. Fifteen-nanometer dots spaced ~ 5 nm apart in the form of an “N” on an Au(111) substrate.

Figure 18. Letter and nanodot writing capabilities of DPN.

This can be viewed as transitioning DPN from a “black and white” to a multi-ink “four-color” type of printing process. How is it done? In DPN, like any scanning probe microscope experiment, locating an initially deposited nanostructure after the sample has been removed from the instrument can be a rather tedious process. However, a postdoctoral associate, Seunghun Hong, developed a type of road map on the surface, generated via DPN, that allows one to get back to an initial nanostructure very easily. This allows us to interchange “ink cartridges” and generate multiple structures, which differ in chemical composition but are perfectly aligned. Figure 20B shows interdigitated lines of octadecanethiol and 16-mercaptohexadecanoic acid. Figure 20C illustrates a technique which I think could have a big impact on molecule-based electronics. We call it over-

writing, and it involves generating one type of structure with one molecule type, and then raster scanning over it with a tip coated with another type of ink. Because the driving force for the writing process is chemisorption, the second ink ignores the areas where the original ink was deposited. It effectively caps off the area surrounding the first nanostructure with the second ink. Recall that the ink transport and chemisorption is taking place in water, so the rate of adsorbate–ink exchange is very slow. The reasons these techniques will be so useful for those in the field of molecule-based electronics is that they allow one to generate very sophisticated architectures and interface them with macroscopically addressable, microscopic circuitry. I firmly believe that DPN will become one of the enabling tools for the scientist interested in nanoscale, molecule-based electronic measurements. It should allow us and others to make many interesting molecule-based architectures very quickly and evaluate their chemical and physical properties as well as their technological potential.

Figure 21 demonstrates the current DPN line width resolution limit, at least with conventional tips. This is a nanostructure made of 16-mercaptohexadecanoic acid. Here, we have used DPN to generate a structure with a 70-nm feature size and 15-nm line width. How small is this structure? If we estimate five letters to a word, one-letter spacing, and 250 words per page, then this degree of resolution enables one to write 80 million pages in a square inch. Although this indicates the amount of information we could potentially store using this technique, it also shows the limitation of the technique in its current state.

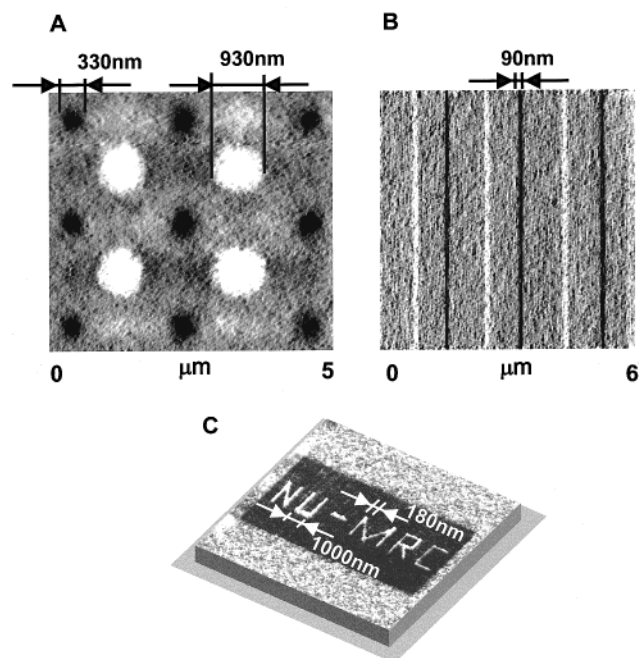


Figure 20. AFM images showing the multiple ink capabilities of DPN. (A) Interdigitated dots of octadecanethiol (black) and 16-mercaptohexadecanoic acid (white). (B) Interdigitated lines of octadecanethiol (black) and 16-mercaptohexadecanoic acid (white). (C) Overwriting. The “NU-MRC” is made of 16-mercaptohexadecanoic acid (white), and the surrounding area is composed of octadecanethiol (dark).

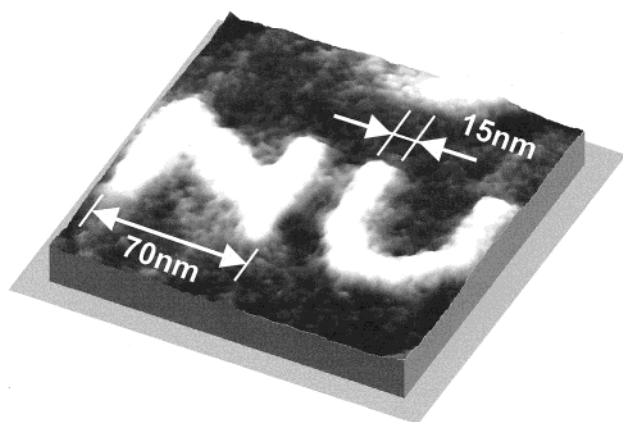


Figure 21. Ultrahigh-resolution DPN on an Au(111) substrate. The “NU” is made of 16-mercaptohexadecanoic acid.

This is a serial method, so at present, it is a customization tool and not one that can be used for mass production. Nevertheless, DPN is a tool that anyone with an AFM can immediately take advantage of to generate and study ultrasmall lithographically patterned structures made of virtually any type of organic molecule. I predict that, in the very near future, we and others will be using DPN to generate customized stamps that can be used for mass producing, in parallel fashion, molecule-based nanoscale architectures that canvas macroscopic dimensions.

DPN offers the following attributes: direct writing, 15-nm line-width resolution, and approximately 5-nm spatial resolution. A key feature of this technique is that writing and imaging are done with the same tool, allowing us to avoid the problem of nanostructure registration. Although, for hard materials, this type of resolution might be possible with e-beam lithography, the AFM used to do DPN is a much simpler tool than an e-beam writer and is accessible to virtually all scientists. DPN is both

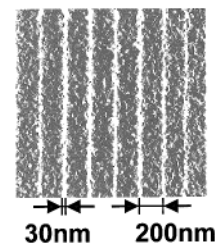


Figure 22. Thirty-nanometer-wide lines of an alkanethiol-functionalized oligonucleotide drawn on a gold substrate via DPN.

substrate and molecule general, and therefore, it allows one to integrate multiple chemical and biochemical functionalities on one nanochip. Finally, DPN is a monolayer process, which can be an advantage or disadvantage, depending upon its intended use. Our group favors such a process because most of the research we do deals with monolayer-modified surfaces and interfaces.

I want to conclude with an especially exciting result, which provides a glimpse into the future for both of the projects that I discussed today. Using a 12-nucleotide sequence functionalized in the 3' end with an alkanethiol, we have been able to generate 30-nm-wide lines of chemisorbed DNA on a gold substrate (Figure 22). The fascinating implication of this experiment is that each one of these lines could be a different type of DNA molecule, suggesting that we should be able to encode a surface with a tremendous amount of information. That information comes in the form of the pattern that we generate via DPN as well as the sequences that comprise the pattern. The idea here is that we can generate a nanotemplate that can guide the assembly of many of the oligonucleotide-functionalized building blocks that we discussed at the beginning of this presentation. This is a chemist's way of programming the formation of any desired nanoparticle-based architecture. This should allow us to explore and discover the properties of these materials when configured into virtually an infinite number of possible two-dimensional structures.

Although I do not profess to be able to predict the future, I think it is likely that DPN will make a big impact in several areas. In view of the resolution offered by DPN and its compatibility with biomolecules, diagnostics and molecule-based electronics are two obvious impact areas. In addition, however, DPN also should enable advances in other areas like catalysis and photonic band-gap materials based upon colloidal crystals. Indeed, Dr. Pierre Wiltzius (Lucent Technologies) and I are exploring the use of DPN for templating the formation of photonic band gap quality, non-fcc colloidal crystals. With regard to catalysis, the spatial resolution of DPN suggests that it might someday be possible to literally draw catalysts, composed of at least two materials, on a surface. Indeed, it is now possible to look at how two lines of molecules (or particles), separated by a predetermined distance, can activate small molecules between them. As the resolution of DPN increases, our power to look at the consequences of miniaturization also will increase. Finally, we are in the process of writing the appropriate software code that can be used to drive the DPN process. When such software is merged with scanning probe instruments that have multiple individually addressable tips, we will have the basis for a many-pen, many-ink nanoplotter. Multipen plotters were work-horse instruments for many years for those who utilized them in the macroscopic world, and I predict that nanoplotters, based upon DPN or some variant of

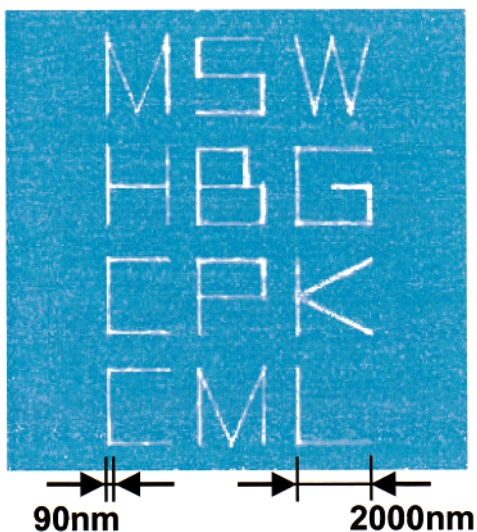


Figure 23. Nanostructure acknowledgment to nominating group written, using DPN, with 16-mercaptohexadecanoic acid as the ink and overwritten with 1-octadecanethiol.

it, will become workhorse instruments in the very near future for those interested in nanotechnology. I will leave you with

those thoughts, but before doing so, I'd like to acknowledge a few people who made this work possible and helped organize this awards address.

Acknowledgment. I wish to thank the ACS and Sigma Xi for this wonderful experience and great honor. I am very pleased to be here and accept the award. I also would also like to thank the many students and postdoctoral associates who have contributed to this work over the past several years. In addition, I am very grateful to those who nominated me for this award. They include Mark S. Wrighton, Harry B. Gray, Clifford Kubiak, and Charles Lieber (Figure 23). The following funding agencies have been very generous in support of our work: the Air Force Office of Scientific Research, the Army Research Office, the National Institutes of Health, the National Science Foundation, and the Office of Naval Research. A special debt of gratitude goes out to Dr. Gary Long of the Naval Medical Research Institute, who provided us with a sample of the anthrax PCR product, and Dr. James Storhoff, who did a tremendous amount of work associated not only with these projects but also with the preparation of this manuscript.

IC991123R